
Omitted Labels in Causality: A Study of Paradoxes

Bijan Mazaheri*

Eric and Wendy Schmidt Center
Broad Institute of MIT and Harvard
Cambridge, MA 02142
bmazaher@broadinstitute.org

Siddharth Jain

Department of Electrical Engineering
California Institute of Technology
Pasadena, CA
sidjain@caltech.edu

Matthew Cook

Cortical Computation Group
ETH Zürich
Zürich, Switzerland
cook@ini.ethz.ch

Jehoshua Bruck

Department of Electrical Engineering
California Institute of Technology
Pasadena, CA
bruck@paradise.caltech.edu

Abstract

We explore what we call “omitted label contexts,” in which training data is limited to a subset of the possible labels. This setting is common among specialized human experts or specific focused studies. We lean on well-studied paradoxes (Simpson’s and Condorcet) to illustrate the more general difficulties of causal inference in omitted label contexts. Contrary to the fundamental principles on which much of causal inference is built, we show that “correct” adjustments sometimes require non-exchangeable treatment and control groups. These pitfalls lead us to the study networks of conclusions drawn from different contexts and the structures the form, proving an interesting connection between these networks and social choice theory.

1 Introduction

Knowledge is powered and limited by the data that drives it. When seeking to understand the relevance of a study, the most important aspect is the *context* of its data. Two common “data contexts” are (1) the population of participants and (2) interventions made on that population. Optimizing a context for utility might involve a census of the target population with perfectly focused interventions. The real world, however, weighs utility against feasibility; budget constraints limit a study’s participants and moral constraints limit its interventions.

Domain Adaptation In the face of these constraints, a study may attempt to transfer conclusions from a sub-optimal *data context* to a *target* one. Most broadly, this topic is known as domain adaptation (DA). DA formally deals with transferring from a training probability distribution $p(\mathbf{V})$ to a target distribution $q(\mathbf{V})$. For a specific training task, we often separate the measured variables into $\mathbf{V} = (Y, \mathbf{X})$, where Y is the “label” and \mathbf{X} are the “covariates.”

DA is made possible through assumptions on the shared information between p and q . Two such assumptions are *covariate shift* [Shimodaira, 2000] and *label shift* [Schweikert et al., 2008].

Another setting that can be considered to fall within DA is causal inference, which seeks to identify the effects of intervening on a variable (often a treatment) without actually performing that intervention [Pearl, 2009, Imbens and Rubin, 2015, Peters et al., 2017]. From a DA perspective, our data-context is “observational” and our target context is “interventional,” i.e. $q(\mathbf{V}) = p(\mathbf{V} \mid \text{do}(T = t))$ for $T \in \mathbf{V}$.

*Work primarily done during Ph.D. at Caltech. <http://bijanmazaheri.com>

Interventional distributions differ from observational ones in that an intervened variable (such as T) contains no information about its usual causes. This property ensures that any outcome differences in Y can be attributed solely to the intervened values rather than spurious correlations. To see this practically, consider the fact that more severe cases of a disease are often treated at higher rates than less severe ones. On average, treated patients may recover at a lower rate than the untreated ones due to the disparity in the severity of their diseases. This differs from the interventional distribution, which would show the individual improvements from treatment.

The best way to learn the causal effects is to perform interventions in a clinical “randomized controlled trial” (RCT). RCTs utilize a random partition into *treatment* and *control* groups, which ensures that no potentially relevant factors (like severity) can effect the probability of receiving treatment. This “exchangeability” between treatment and control forms a key principle of the interventional distributions that causal inference aims to emulate.

A common technique within DA is to transform the data’s distribution to the target context through importance weighting. These weights make up for poorly represented portions of a data distribution by giving them more importance. For label shift, this corresponds to weighting data by the ratio of label probabilities ($w(\mathbf{x}, y) = q(y)/p(y)$). Similarly, covariate shift can be accounted for using a ratio of covariate probabilities ($w(\mathbf{x}, y) = q(\mathbf{x})/p(\mathbf{x})$). Causal inference performs similar reweightings to transform observational data into distributions with exchangeable treatment and control groups, the most obvious of which is “inverse propensity weighting” [Imbens and Rubin, 2015, Cole and Hernán, 2008, Hernán MA, 2020]. Covariate adjustment techniques like the “backdoor adjustment” [Pearl, 2009] and “G-computation” [Robins et al., 2009] perform adjustments at the distribution level that can nonetheless be thought of as reweighting data.

Omitted Label Contexts This paper will discuss a relatively new branch of the DA tree introduced by Mazaheri et al. [2021], which we will call “omitted label contexts.” Such settings are limited to *only a subset* $\mathcal{Y}^* \subset \mathcal{Y}$ of the labels for $Y \in \mathcal{Y}$. For example, “dogs vs. cats” is omitted label context, but “dogs vs. non-dogs” is not. While the relative probabilities of classes within this subset are maintained, data from all other labels are unobserved. More precisely, $p(y_1^*)/p(y_2^*) = q(y_1^*)/q(y_2^*)$ for $y_1^*, y_2^* \in \mathcal{Y}^*$, but $p(y') = 0$ if $y' \notin \mathcal{Y}^*$. Within the scope of this paper, we will restrict our focus to $|\mathcal{Y}^*| = 2$.

Omitted label contexts are motivated by a few real-life scenarios within medicine and epidemiology. The first is “immortal time bias” [Suisa, 2008], which famously reversed the perceived risks of postmenopausal hormone treatment. While initial observational studies suggested this treatment could decrease in cardiovascular issues [Grodstein et al., 2006], a followup clinical study eventually showed the opposite [Michels and Manson, 2003].² This discrepancy can be attributed to the observational study’s focus on *current users* of the therapy [Hernán et al., 2008]. More specifically, the backtracking nature of the observational study excluded a group of vulnerable women who had not survived treatment long enough to participate – i.e. all participants were “immortal” from the inception of their treatment to the beginning of the study. Exclusion of an outcome (in this case, death before the study) constitutes an example of a omitted label context.

Omitted label contexts are also extremely common in the study of rare conditions. For example, a census genome sequencing of the US population would be an impractical and financially infeasible task. Instead, databases like TCGA [Tomczak et al., 2015] allow focused access to patients with specific (and often rare) cancers. In study designs, investigators may opt for an omitted label context or induce further label shift by working with a uniform distribution on the labels of interest.

Omitted labels are a form of sampling bias – a topic that has been studied in detail within the causal inference literature [Bareinboim and Tian, 2015, Correa et al., 2019]. Bareinboim and Tian [2015] calls a causal effect “recoverable” if it can be computed in the presence of a selection mechanism. An important difficulty within omitted label contexts is that they are what we will call “irreversible.” Zero-probability labels cannot be “weighted-up” to transform the distribution to the that of the general population. With respect to covariate adjustments, this leads to incompatible quantities that make the causal effects unrecoverable.

Contributions This paper will begin by illustrating the potentially severe consequences omitted label bias, particularly with respect to unrecoverable causal effects. We consider what happens when

²Grodstein et al. [2006] was initially published before Michels and Manson [2003], but later updated.

these effects are ignored, demonstrating that omitted labels can give rise to reversals in calculated treatment effects, as in Simpson’s paradox. This paradox is driven by the non-exchangeability of “correct” causal inference weights in omitted label contexts. This means that standard adjustments to exchangeability give us incorrect quantities.

The problems that arise within omitted label contexts are of no surprise – the task computing unrecoverable causal effects is bound for failure. However, within the details of these failures emerges an interesting structure between the conclusions of multiple (erroneous) studies with *different* restrictions on their labels. Specifically, a “new”³ paradox manifests within the combination of erroneous causal conclusions. We will link this paradox to a 200-year-old observation from social choice theory known as the “Condorcet paradox,” which demonstrates how ranked-choice votes (i.e. an preference ordering of the candidates for each voter) can result in a cycle of aggregate preference [Nicolas et al., 1785]. In a surprising connection between social choice theory, causality, and machine learning, we prove that these phenomena are one in the same.

The task of combining conclusions from different models is sometimes referred to as decision fusion [Castanedo, 2013]. The usual reasons for studying decision fusion involve lack of access to data or inability to combine datasets (e.g. because of non-overlapping covariates). As advances in large models (such as LLMs) transition us from data-based to model-based vehicles of information, studying how to fuse decisions from multiple models will be of growing importance.

Summary Section 2 begins by explaining Simpson’s paradox through an example that will be expanded on throughout the paper. Section 3 studies omitted label contexts and shows how and why they can exhibit Simpson’s paradox in causality. Section 4 introduces Condorcet’s paradox and the linear ordering polytope and shows their relationship to networks of conclusions from different omitted label contexts. Section 5 concludes the paper and discusses its implications.

Notation In general, we will use the capital Latin alphabet (i.e. X, Y, T) to denote random variables, with Y being the “label” or class we wish to predict or determine the causal effect on, X being the covariates, and T being the treatment. The lowercase Latin alphabet will denote assignments to these variables, e.g. $x^{(1)}$ means $X = x^{(1)}$. Vectors and sets of random variables will be in bold-face font, while other types of sets will use calligraphic font (i.e. $\mathcal{Y} = \{y^{(1)}, y^{(2)}, \dots\}$). The following notation is used throughout the paper.

- $\Pr(\cdot)$ will be used for probability. $p(\cdot)$ and $q(\cdot)$ will also be used when discussing DA.
- $\mathbf{1}^\ell$ denotes an all 1 vector of size ℓ .
- Δ^ℓ denotes the space of vectors of length ℓ in the simplex (e.g. probability distributions). That is, $\lambda \in \Delta^\ell$ iff $\lambda \in [0, 1]^\ell$ and $\mathbf{1}^\top \lambda = 1$.
- $<$ and \leq denote element-wise inequality. For example, we say $\mathbf{w} \leq \mathbf{v}$ if $w_i \leq v_i \forall i \in [\ell]$.
- We will use $\text{Co}(S)$ to denote the open convex hull of S , $\overline{\text{Co}}(S)$ to denote the closed convex hull, and $\text{Bo}(\cdot)$ to denote the boundary.

2 Simpson’s Paradox

We will ease into our dissection of errors in causal quantities by discussing Simpson’s paradox. This discussion will rely on a hypothetical observational data on a treatment T and its outcome Y , given in Table 1 (a). The example is motivated by the effect of illness severity on the probability of treatment prescription, as discussed in the introduction. Patients improve with treatment within both severe and mild cases, but treatment is primarily given to more severe illnesses that have a lower overall rate of improvement. As a result, treated patients have a lower rates of improvement than untreated patients.

The driver for Simpson’s paradox is the difference in severity between those who did and did not receive treatment, and the effect of this severity on patient outcomes. That is to say the treatment and control groups are not exchangeable. A natural solution to this is to reweight the rows of our table to exchangeability by emphasizing the severely ill patients who did not receive treatment and the

³The paradox is very similar to the one introduced in Mazaheri et al. [2021], but has not been observed for causality of covariate shift.

T	X	$y^{(0)}$	$y^{(1)}$
$t^{(0)}$	$x^{(0)}$	3	7
$t^{(0)}$	$x^{(1)}$	1	0
$t^{(1)}$	$x^{(0)}$	0	1
$t^{(1)}$	$x^{(1)}$	7	3

(a) A specification of counts for Simpson’s Paradox.

T	X	$y^{(0)}$	$y^{(1)}$	$y^{(2)}$
$t^{(0)}$	$x^{(0)}$	3	7	0
$t^{(0)}$	$x^{(1)}$	1	0	99
$t^{(1)}$	$x^{(0)}$	0	1	99
$t^{(1)}$	$x^{(1)}$	7	3	0

(b) An augmentation of (a) with a third column that shifts the distribution of X .

T	X	$y^{(0)}$	$y^{(1)}$	$y^{(2)}$
$t^{(1)}$	$x^{(0)}$	2	1	0
$t^{(1)}$	$x^{(1)}$	0	2	1
$t^{(1)}$	$x^{(2)}$	1	0	2
$t^{(0)}$	$x^{(0)}$	0	1	2
$t^{(0)}$	$x^{(1)}$	2	0	1
$t^{(0)}$	$x^{(2)}$	1	2	0

(c) A specification of counts that mimics Condorcet’s paradox.

Table 1: Three tables discussed in this paper.

mildly ill patients who did receive treatment. This is accomplished by reweighting datapoints (t, x, y) according to the inverse propensity of receiving the treatment that they got, $w(t, x, y) = 1/\Pr(t | x)$, sometimes referred to as “Inverse Propensity Weighting” (IPW) [Imbens and Rubin, 2015]. For Table 1 (a), this corresponds to weighting up the second and third rows by a factor of 10. When this reweighting is interpreted as a synthetic study on 40 participants (20 treated and 20 control, each with a 10 : 10 split on severity), the new apparent treatment effect is $13/20 - 7/20 = 30\%$.

An alternative perspective is that the causal effect of the treatment lies in the outcome changes *within each severity group*. By separately considering the severe and mild patients, we can average outcomes according to the marginal probability distribution of severity. Following this intuition, the “backdoor adjustment” [Pearl, 2009] calculates the probability distribution of $Y = y^{(i)}$ under an intervention of $T = t^{(j)}$:

$$\Pr(y^{(i)} | \text{do}(t^{(j)})) := \sum_x \Pr(x) \Pr(y^{(i)} | x, t^{(j)}).$$

The difference between the two possible interventions gives the “average treatment effect” (ATE),

$$\text{ATE} = \Pr(y^{(1)} | \text{do}(t^{(1)})) - \Pr(y^{(1)} | \text{do}(t^{(0)})) = \frac{1/1 + 3/10}{2} - \frac{7/10 + 0/1}{2} = .3.$$

Notice that the marginal probability distribution of X is uniform, corresponding to an equal weighting of the $x^{(0)}$ and $x^{(1)}$ rows in Table 1 (a). In fact, both IPW and backdoor approaches result in the same weightings of the rows of the table because $\Pr(t, x)/\Pr(t | x) = \Pr(x)$.

Simpson’s paradox has been the subject of a long list of works for which it would be impossible to do a full justice to. Pearl [2022] and Hernán et al. [2011] describe Simpson’s paradox as “solved” by causal modeling because the confounding role of X tells the researcher how to proceed, namely that they must separately consider outcome changes for each assignment of x . We will focus on one key takeaway: the choice of how to re-weight sub-cases (rows of our table) plays a key role in the conclusion of a study, sometimes reversing the apparent relationship (as in Simpson’s Paradox).

An important observation that there is a geometry to the way in which these errors occur. Notice that the reversal in Table 1 (a) would be maximized by further increasing the probability of rows 1 and 4, e.g. by changing the 3, 7 counts to 300, 700. This reweighting strengthens the dependence of T on X , resulting in an unadjusted treatment effect that approaches $\Pr(y^{(1)} | t^{(1)}, x^{(1)}) - \Pr(y^{(1)} | t^{(0)}, x^{(0)}) = .4$. While we will not dive further into the geometry of Simpson’s paradox, the existence of this structure stands as motivation for the structures we will study within networks of contexts.

3 Omitted Label Contexts

Now that we understand the potential effects of reweighting distributions on covariates, we will move our focus to the study of omitted label contexts. As discussed in the introduction, omitted label contexts involves the removal of some labels while preserving the relative probabilities of the non-removed labels. This removal can shift the apparent distribution of any variable that is associated with Y , including both treatment T and covariates X .

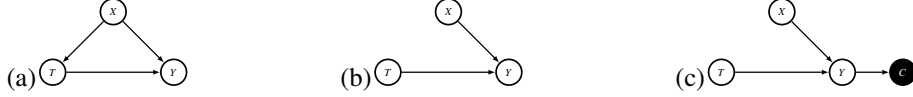


Figure 1: (a) A causal DAG depicting confounding from a common cause X . (b) The causal DAG that “severs” $X \rightarrow T$ by reweighting for exchangeability. (c) The causal DAG depicting the effect of an omitted label context C which has been conditioned on.

3.1 Causality within Omitted Label Contexts

Consider a second hypothetical dataset that augments Table 1 (a) with an additional column, shown in Table 1 (b). We will focus on the context that excludes the deceased ($y^{(2)}$) label, meaning that the observed dataset is equivalent to Table 1 (a), which we recall has a .3 ATE on the outcome of $y^{(1)}$. Although the full context has the exact same (uniform) marginal probability distribution on X , we see a reversal of the ATE on $y^{(1)}$:

$$\text{ATE} = \frac{1/100 + 3/10}{2} - \frac{7/10 + 0/100}{2} = -.195. \quad (1)$$

The correct adjustment comes down to a loss of datapoints. The goal is to shift to exchangeable treatment and control distributions in the *overall population*, which involves weights $w(t^{(0)}, x^{(0)}, y) = w(t^{(1)}, x^{(1)}, y) = 10$ and $w(t^{(0)}, x^{(1)}, y) = w(t^{(1)}, x^{(0)}, y) = 1$, or any other rescaling. Notice that this reweighting differs from the reweighting suggested by IPW and the backdoor adjustment in the left table. Instead of scaling up the $(t^{(1)}, x^{(0)})$ and $(t^{(0)}, x^{(1)})$ rows to make up for a bias towards giving treatment to more severe cases, the correct reweighting does the opposite, resulting in a seemingly less exchangeable distribution.

This effect can be understood by graphically the selection bias as in Bareinboim and Tian [2015], shown in Figure 1. Figure 1 (a) shows the graph describing a confounding variable X causing both T and Y . The goal of IPW and the backdoor adjustment is to reweigh the distribution to fit the DAG in Figure 1 (b), i.e. a distribution in which the distribution of X is exchangeable in both $t^{(0)}$ and $t^{(1)}$ or equivalently $X \perp\!\!\!\perp T$. Figure 1 (c) shows the effect of restricting the labels of Y within a dataset context (such as with omitted label contexts), which involves conditioning on a child of Y . X and T are not d -separated⁴, because conditioning on a variable that is causally downstream of both X and T can induce a correlation.

The effect we have outlined darkens the outlook for causal inference in omitted label contexts: We are no longer guided by the principle of exchangeability in our observed data and finding the correct adjustment requires knowledge of the context-induced distribution $\Pr(X, T, Y \mid y \in \{y^{(i)}, y^{(i)}\})$. This distribution cannot be obtained without extending the study to all labels.

We now investigate what can be learned from many conclusions under *different* omitted label contexts. Such a network is not a replacement for a single study on all of the potential labels, but is a realistic setting for patching omitted label bias. We study networks of conclusions that ignore the limitations of their omitted labels and perform standard adjustments. We will see that these networks have limitations, much like the limitations to Simpson’s paradox.

4 Networks of Contexts

Before we discuss the structures within networks of omitted label contexts, we will introduce another paradox from social choice theory, known as the Condorcet Paradox [Nicolas et al., 1785]. We will see that this paradox and its structure are deeply related to the networks we will study.

4.1 The Condorcet Paradox

The Condorcet paradox works as follows: three voters each have preferences $y^{(0)} \rightarrow y^{(1)} \rightarrow y^{(2)}$, $y^{(1)} \rightarrow y^{(2)} \rightarrow y^{(0)}$, and $y^{(2)} \rightarrow y^{(0)} \rightarrow y^{(1)}$, with $a \rightarrow b$ indicating a preference of a over b . The key to these preferences is that the order has been rotated three times, meaning that each candidate

⁴see Pearl [2009] for the full rules of d -separation

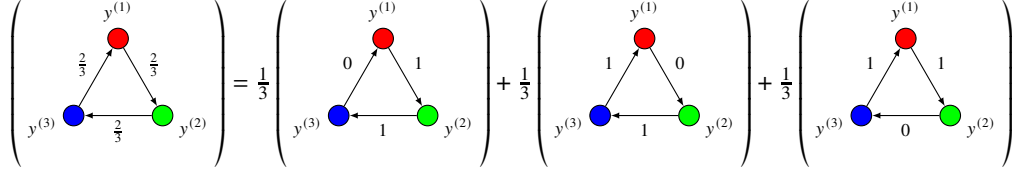


Figure 2: The Condorcet paradox as an aggregation of rankings.

is preferred to its successor mod 2. That is, $y^{(i)} \rightarrow y^{(i+1 \bmod 2)}$ in two out of the three voters. The result is an aggregate cycle of preference $y^{(0)} \rightarrow y^{(1)} \rightarrow y^{(2)} \rightarrow y^{(0)}$ with frequencies of $2/3$ voters for each edge.

This paradox can be generalized into what we will call an “aggregation of rankings” (AR) – a complete directed-graph⁵ on the set of labels \mathcal{Y} with weights on each $y^{(i)} \rightarrow y^{(j)}$ corresponding to the fraction of voters who prefer $y^{(i)}$ to $y^{(j)}$. AR structures are a convex combination of total orderings (i.e. graphs with edge weights of 0 or 1), with component weights corresponding to the fraction of voters carrying each total ordering. See Figure 2 for an illustration of this perspective for the Condorcet paradox. As a result, the space occupied by all possible AR structures is known as the “linear ordering polytope,” which has been the subject of extensive study [Fishburn, 1992, Alon, 2002].

The preferences of voters in the Condorcet paradox can be embedded into a table of frequencies, with each voter becoming a specific value for covariate X . Table 1 (c) demonstrates this using the counts $2 > 1 > 0$ to induce high, medium, and low preference. Notice that the order of preferences for each x in the $t^{(1)}$ half of the table (first three rows) exactly correspond to the order of preferences given by the voters in the Condorcet paradox, starting with $y^{(0)} \rightarrow y^{(1)} \rightarrow y^{(2)}$ for $x^{(0)}$ and cycling the order with the other values of X .

The $t^{(0)}$ half of the table complements the $t^{(1)}$ half so that the counts for $(t^{(0)}, x^{(i)}, y^{(j)})$ and $(t^{(1)}, x^{(i)}, y^{(j)})$ always sum to three. As a result, restricting our table to any two columns still yields a uniform probability distribution on X , i.e. $\Pr(x^{(0)} \mid y \in \{y^{(i)}, y^{(j)}\}) = \Pr(x^{(1)} \mid y \in \{y^{(i)}, y^{(j)}\}) = \Pr(x^{(2)} \mid y \in \{y^{(i)}, y^{(j)}\})$. This is the distribution that a naive study would average over when applying a backdoor adjustment, meaning that

$$\begin{aligned} \Pr(y^{(0)} \mid \text{do}(t^{(1)}), y \in \{y^{(0)}, y^{(1)}\}) &= \frac{2/3 + 0/2 + 1/1}{3} = 5/9 \\ \Pr(y^{(0)} \mid \text{do}(t^{(0)}), y \in \{y^{(0)}, y^{(1)}\}) &= \frac{0/3 + 2/2 + 1/3}{3} = 4/9. \end{aligned} \tag{2}$$

The calculations in 2 conclude that the ATE on $y^{(0)}$ in the $y \in \{y^{(0)}, y^{(1)}\}$ context is $+1/9$. These calculations are the same for the ATE on $y^{(1)}$ for $y \in \{y^{(1)}, y^{(2)}\}$ and the ATE on $y^{(2)}$ for $y \in \{y^{(2)}, y^{(0)}\}$ due to the cyclic shifting of columns. Hence, the studies separately conclude that the treatment increases the relative frequency of all three labels, which is clearly impossible.

The embedding of the Condorcet paradox into causal conclusions implies a correspondence between aggregations of rankings and backdoor adjustments⁶.

Cardinal vs Ordinal Systems The Condorcet paradox is primarily driven by the loss of information in an ordinal system. That is, an ordering of $A \rightarrow B \rightarrow C$ cannot distinguish between the magnitude of the preferences $A \rightarrow B$ and $A \rightarrow C$. If voters were instead allowed to allocate multiple votes among the candidates (e.g. one voter gives 2 votes for A , 1 for B , and 0 for C), it would be clear that $A \rightarrow C$ is a stronger opinion than $A \rightarrow B$ (that is, $2 - 1 < 2 - 0$). Indeed, such “cardinal” voting systems do not give rise to paradoxes of transitivity [Conklin and Sutherland, 1923].

The paradox we have constructed is based on a probability distribution on the labels, which is a cardinal data-type. Hence, it is surprising that we will show these two paradoxes to both occupy the

⁵These graphs are always complete, but we use graph terminology as in Mazaheri et al. [2021] in order to reference properties that are dependent on cycles.

⁶or any other case-based weighting

linear ordering polytope. That is, for every instance of a network of do-interventions⁷ (computed within different overlapping omitted label contexts), there exists a population of orderings that also yields those same numbers as their aggregate preferences, and vice versa. We will call these two structures “aggregations of soft rankings” and “aggregations of rankings,” which we will now define.

4.2 Aggregations of Rankings and Soft Rankings

Table 1 (c) used counts of 2, 1, 0 to induce preference between labels in each row. As this system is effectively cardinal, these preferences differ from those in the Condorcet paradox in that they can be any frequencies between $[0, 1]$. For this reason, we refer to the induced preferences in each row of our tables as a “soft ranking.” We will now be formal about both aggregations of rankings (ARs) and aggregations of soft rankings (ASRs).

Definition 1 (Ranking). A ranking of \mathcal{Y} is a function $A : \mathcal{Y} \times \mathcal{Y} \rightarrow \{0, 1\}$ generated by a total ordering. We use $A(y^{(i)}, y^{(j)}) = 1$ to denote preference $y^{(i)} \rightarrow y^{(j)}$ and $A(y^{(i)}, y^{(j)}) = 0$ for $y^{(i)} \leftarrow y^{(j)}$.

Definition 2 (Aggregation of Rankings (AR)). An aggregation of rankings is specified by a set of rankings \mathbf{A} and a corresponding weight function $\alpha \in \Delta^{|\mathbf{A}|}$ (indexed by $A \in \mathbf{A}$).

Definition 3 (Aggregate Preference). An aggregation preference in an AR between $y^{(i)}, y^{(j)} \in \mathcal{Y}$ is defined to be

$$R_{\mathbf{A}, \alpha}(y^{(i)}, y^{(j)}) := \sum_{A \in \mathbf{A}} \alpha_A A(y^{(i)}, y^{(j)}).$$

Corresponding to rankings, ARs, and aggregate preferences $R_{\mathbf{A}, \alpha}$, we will have soft rankings, ASRs, and aggregate probabilities $F_{\mathbf{B}, \beta}$.

Definition 4 (Soft Rankings). A soft ranking on \mathcal{Y} is a function $B : \mathcal{Y} \times \mathcal{Y} \rightarrow [0, 1]$ generated by a categorical probability distribution on \mathcal{Y} , $\mathbf{p} \in \Delta^{|\mathcal{Y}|}$.

$$B(y^{(i)}, y^{(j)}) := \frac{p_i}{p_i + p_j}.$$

Definition 5 (Aggregation of Soft Rankings (ASR)). An aggregation of soft rankings is specified by a set of soft rankings \mathbf{B} and a corresponding weight function $\beta \in \Delta^{|\mathbf{B}|}$ (indexed by $B \in \mathbf{B}$).

Definition 6 (Aggregate Probability). An aggregate probability in an ASR between $y^{(i)}, y^{(j)} \in \mathcal{Y}$ is

$$F_{\mathbf{B}, \beta}(y^{(i)}, y^{(j)}) := \sum_{B \in \mathbf{B}} \beta_B B(y^{(i)}, y^{(j)}).$$

Observation 1. Suppose the probability distribution for a covariate adjustment on \mathbf{X} (e.g. X in our previous examples), $\Pr(\mathbf{X} \mid Y \in \{y^{(i)}, y^{(j)}\})$ is the same for all pairs of labels $\{y^{(i)}, y^{(j)}\}$. The treatment effects computed for each label pair then correspond to the difference between the aggregate probabilities in two ASRs with a B for each assignment of $\mathbf{X} = \mathbf{x}$ and $\beta_B = \Pr(\mathbf{x} \mid Y \in \{y^{(i)}, y^{(j)}\})$.

The remainder of this paper will be dedicated to showing that ARs and ASRs on the same cardinality $|\mathcal{Y}| = n$ can hold the exact same vectors of weights. To make this statement precise, we will denote \mathcal{R} as the set of $\{0, 1\}^{n(n-1)}$ vectors associated with the output values of some A in a total ordering and $\text{Co}(\mathcal{R})$ as its convex hull. Note that $\text{Co}(\mathcal{R})$ is the space of possible vectors of aggregate preferences $R(y^{(i)}, y^{(j)})$. Similarly denote \mathcal{B} as the set of $[0, 1]^{n(n-1)}$ vectors generated by some categorical distribution and note its convex hull $\text{Co}(\mathcal{B})$ is the space of possible aggregate probability vectors.

Theorem 1. $\text{Co}(\mathcal{R})$ and $\overline{\text{Co}(\mathcal{B})}$ are the same.

It is not difficult to see how soft rankings can be made “harder” by simply increasing the relative difference in counts. That is, replacing 2, 1, 0 in Table 1 (c) with 100, 1, 0 more closely simulates an absolute preference. Showing that any set of aggregate probabilities from an ASR can be realized with aggregate preferences from an AR is less obvious. We will prove this direction by using the probability table in an ASR to directly construct a corresponding AR.

⁷Note here that we are now just studying the do-intervention rather than the ATE, which is the difference between two do-interventions.

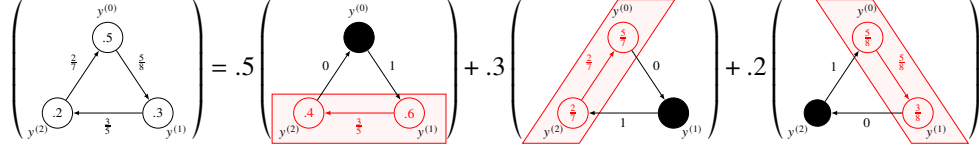


Figure 3: A demonstration of the inductive step in the proof for Lemma 3. The weights on the LHS are the aggregate probabilities $(y^{(i)}, y^{(j)})$ that we wish to generate, while the numbers within each vertex $y^{(i)}$ specify p_i . The weights of the graphs on the RHS are given by Equation 4, with adjusted (re-normalized) probabilities $p^{[l-k]}$ specified within the vertices. Three subgraphs are highlighted in red, which represent the smaller sets of labels which can be decomposed according to the inductive hypothesis.

4.3 Probabilities can Emulate Preferences

We will begin with the simpler direction, given by Lemma 1.

Lemma 1. $Co(\mathcal{A}) \subset \overline{Co(\mathcal{B})}$.

To prove Lemma 1, we will first show that for every $A \in \mathcal{A}$, there exists a $B \in \mathcal{B}$ which is arbitrarily close to it. We will then make use of the following more general lemma, which we prove in Appendix A.

Lemma 2. Consider a set of vectors $V = \{\mathbf{v}_1, \dots, \mathbf{v}_t\}$ and with $\mathbf{v}_i \in \mathbb{R}^m$ for all i . If we have \tilde{V} such that for every $\varepsilon > 0$ and $\mathbf{v} \in V$, there exists $\tilde{\mathbf{v}} \in \tilde{V}$ such that $\|\tilde{\mathbf{v}} - \mathbf{v}\|_2 < \varepsilon$, then $Co(V) \subseteq \overline{Co(\tilde{V})}$.

We now give the proof for Lemma 1.

Proof. For a given A from a total ordering, we will show how to find a probability vector \mathbf{p} that generates a B with values that are arbitrarily close to the 0, 1 values of A . As already alluded to, this will involve blowing up the ratios of the probabilities in \mathbf{p} .

Let $y^{(0)} \rightarrow \dots \rightarrow y^{(n-1)}$ be the ordering specified without loss of generality. Let the i th element of \mathbf{p} be ε^i/z , where $z = \sum_{j=1}^n \varepsilon^j$ is simply a normalization factor so that \mathbf{p} remains in the simplex. Notice that this assignment gives us

$$B(y^{(i)}, y^{(j)}) = \frac{1}{1 + \varepsilon^{j-i}}$$

for all $j > i$. Our goal is $B(y^{(i)}, y^{(j)})$ arbitrarily close to $A(y^{(i)}, y^{(j)}) = 1$ for $j > i$. Setting $\varepsilon > 0$ arbitrarily close to 0 achieves this. Finally, we can apply Lemma 2 to complete our proof. \square

4.4 Preferences can Emulate Probabilities

We will continue with the more difficult direction, given by Lemma 3.

Lemma 3. $Co(\mathcal{B}) \subset Co(\mathcal{A})$.

We will prove this direction by showing that every possible instance of B is in $Co(\mathcal{A})$. Convexity of $Co(\mathcal{A})$ will then complete the proof.

Let $\mathbf{A}^{(i)} \subset \mathbf{A}$ denote the set of rankings for which $y^{(i)}$ is the “first choice.” Equivalently, $\mathbf{A}^{(i)}$ is defined such that we have $A(y^{(i)}, y^{(j)}) = 1$ for all $j \neq i$ and $A \in \mathbf{A}^{(i)}$. We extend this notation to multiple indices, with $\mathbf{A}^{(ij)}$ encoding $y^{(i)}$ as first choice and $y^{(j)}$ as second choice. If the number of rankings that satisfy the restriction is singular, then we remove the bold, e.g. $A^{(ij)}$.

Proof. We will induct on the number of labels n . The inductive hypothesis is that any $B \in \mathcal{B}$ generated by a categorical distribution $\mathbf{p} \in \Delta^n$ over n labels can be expressed as an AR \mathbf{A} , α . This can easily be shown for the base case of $n = 2$ by assigning $\alpha_{A^{(01)}} = p_0$ and $\alpha_{A^{(10)}} = p_1$.

Now, assuming the inductive hypothesis to be correct for all B on n labels, we will show how to construct an AR for a B on $n + 1$ labels.

First, expand $R_{\mathbf{A}, \alpha}$, which we have not yet specified, into aggregate rankings on $\mathbf{A}^{(0)}, \dots, \mathbf{A}^{(n)}$,

$$R_{\mathbf{A}, \alpha} = \sum_{k=0}^n p_k R_{\mathbf{A}^{(k)}, \alpha^{(k)}}. \quad (3)$$

Now, consider choosing some label $y^{(k)}$ and constructing a new $\mathbf{p}^{[-k]} \in \Delta^n$ by setting $p_k^{[-k]} \leftarrow 0$ and all other $p_i^{[-k]} \leftarrow p_i / (1 - p_k)$. Notice that $B(y^{(i)}, y^{(j)})$ is invariant to scaling p_i, p_j (if scaled together). Therefore, this new $\mathbf{p}^{[-k]}$ implies a $B^{[-k]}(y^{(i)}, y^{(j)})$ that matches $B(y^{(i)}, y^{(j)})$ for all $i, j \neq k$. $B^{[-k]}$ also satisfies the requirements for the inductive hypothesis, so we can assume there is a set of rankings $\mathbf{A}^{[-k]}$ and corresponding $\alpha^{[-k]}$ that forms an AR for which $R_{\mathbf{A}^{[-k]}, \alpha^{[-k]}} = B^{[-k]}$.

Each $\mathbf{A}^{[-k]} \in \mathbf{A}^{[-k]}$ can now be augmented with a first-choice preference of $y^{(k)}$ to generate the set $\mathbf{A}^{(k)}$ with corresponding $\alpha^{(k)} = \alpha^{[-k]}$. Using this assignment, we have that

$$R_{\mathbf{A}^{(k)}, \alpha^{(k)}}(y^{(i)}, y^{(j)}) = \begin{cases} B(y^{(i)}, y^{(j)}) & \text{if } i, j \neq k \\ 1 & \text{if } i = k \\ 0 & \text{if } j = k \end{cases} \quad (4)$$

Applying Equation 4 to Equation 3 gives,

$$\begin{aligned} R_{\mathbf{A}, \alpha}(y^{(i)}, y^{(j)}) &= p_i + \sum_{k \neq i, j} p_k B(y^{(i)}, y^{(j)}) = (p_i + p_j)B(y^{(i)}, y^{(j)}) + (1 - p_i - p_j)B(y^{(i)}, y^{(j)}) \\ &= B(y^{(i)}, y^{(j)}). \end{aligned}$$

We chose i, j wlog, so we have constructed an AR which emulates the the soft ranking B . This completes the inductive proof. As stated earlier, convexity of $\text{Co}(\mathcal{A})$ gives the desired result. \square

As the proof for Lemma 3 is rather complicated, Figure 3 illustrates an example inductive step.

5 Discussion

This paper studies dataset contexts and how they affect the conclusions we take from them. Specifically, we have explored how the traditional principles of causal inference break down in omitted label contexts through the manifestation of two well-known paradoxes. These paradoxes warn practitioners that seek to do causal inference within a label-biased setting.

While perhaps limited, we believe that the study of omitted label contexts may have applications towards handling other forms of label bias. In the study of rare diseases, it may be unfeasible to avoid scaling up the proportion affected individuals. This is a form of label bias and comes with all of the caveats discussed in the preceding sections. An intriguing alternative is to instead combine the label of interest with another similarly rare disease. In a dataset of two rare diseases, one can maintain the relative probabilities of the labels while keeping their portion of the dataset nontrivial. In order to extend the results of this type of study to the broader population, one can imagine computing multiple ratios of increasingly more common labels in order to compute the context-induced distributions needed to perform adjustments.

This paper also begins the study of structures that arise when combining conclusions from different omitted label contexts, connecting them to the linear ordering polytope. While the linear ordering polytope has a few counter-intuitive properties, such as the breakdown of preference-transitivity, it also has limitations. For example, the Condorcet paradox actually represents the “maximum amount of nontransitivity” that is possible in a cycle of three choices. It is not possible for a cycle of 80% preferences to exist, nor is a cycle of 100%, 50%, 70% possible. In fact, for any cycle of length ℓ , the aggregate preferences along that cycle must sum to between 1 and $\ell - 1$, a property discussed in Fishburn [1992] as the “triangle inequality” and Mazaheri et al. [2021] as the “curl condition.”

These limitations can be harnessed to provide bounds on unmeasured aggregate preferences, or “missing edge weights” as discussed in Mazaheri et al. [2021]. That is, if we are missing a study

on two labels, we can provide bounds on that study's likely outcome using the outcomes of related studies. Furthermore, we can use these properties to detect inconsistencies within sets of studies.

As larger machine learning models become more costly to train and comprehensive data drifts towards private datasets, many practitioners are choosing to re-purpose pretrained "checkpoints" to new tasks. Of course, these check-points all come from data-contexts. Hence, we see decision fusion from different contexts as an essential upcoming field to launch data-science into a new age.

References

- Noga Alon. Voting paradoxes and digraphs realizations. *Advances in Applied Mathematics*, 29(1):126–135, 2002.
- Elias Bareinboim and Jin Tian. Recovering causal effects from selection bias. In *Proceedings of the AAAI Conference on Artificial Intelligence*, volume 29, 2015.
- Federico Castanedo. A review of data fusion techniques. *The scientific world journal*, 2013.
- Stephen R Cole and Miguel A Hernán. Constructing inverse probability weights for marginal structural models. *American journal of epidemiology*, 168(6):656–664, 2008.
- Edmund S Conklin and John W Sutherland. A comparison of the scale of values method with the order-of-merit method. *Journal of Experimental Psychology*, 6(1):44, 1923.
- Juan D Correa, Jin Tian, and Elias Bareinboim. Identification of causal effects in the presence of selection bias. In *Proceedings of the AAAI Conference on Artificial Intelligence*, volume 33, pages 2744–2751, 2019.
- Peter C Fishburn. Induced binary probabilities and the linear ordering polytope: A status report. *Mathematical Social Sciences*, 23(1):67–80, 1992.
- Francine Grodstein, Joann E Manson, and Meir J Stampfer. Hormone therapy and coronary heart disease: the role of time since menopause and age at hormone initiation. *Journal of Women's Health*, 15(1):35–44, 2006.
- Branko Grünbaum, Victor Klee, Micha A Perles, and Geoffrey Colin Shephard. *Convex polytopes*, volume 16. Springer, 1967.
- Miguel A Hernán, Alvaro Alonso, Roger Logan, Francine Grodstein, Karin B Michels, Walter C Willett, JoAnn E Manson, and James M Robins. Observational studies analyzed like randomized experiments: an application to postmenopausal hormone therapy and coronary heart disease. *Epidemiology*, 19(6):766–779, 2008.
- Miguel A Hernán, David Clayton, and Niels Keiding. The Simpson's paradox unraveled. *International Journal of Epidemiology*, 40(3):780–785, 03 2011. ISSN 0300-5771. doi: 10.1093/ije/dyr041. URL <https://doi.org/10.1093/ije/dyr041>.
- Robins JM Hernán MA. *Causal Inference: What If*. Boca Raton: Chapman & Hall/CRC, 2020.
- G. W. Imbens and D. B. Rubin. *Causal inference in statistics, social, and biomedical sciences*. Cambridge University Press, 2015.
- Bijan Mazaheri, Siddharth Jain, and Jehoshua Bruck. Synthesizing New Expertise via Collaboration. In *2021 IEEE International Symposium on Information Theory (ISIT)*, pages 2447–2452, 2021. doi: 10.1109/ISIT45174.2021.9517822.
- Karin B Michels and JoAnn E Manson. Postmenopausal hormone therapy: a reversal of fortune, 2003.
- Jean Antoine Nicolas et al. *Essai sur l'application de l'analyse à la probabilité des décisions rendues à la pluralité des voix. Par m. le marquis de Condorcet,...* de l'Imprimerie Royale, 1785.
- Judea Pearl. *Causality*. Cambridge university press, 2009.
- Judea Pearl. Comment: understanding simpson's paradox. In *Probabilistic and causal inference: The works of judea Pearl*, pages 399–412. 2022.
- Jonas Peters, Dominik Janzing, and Bernhard Schölkopf. *Elements of causal inference: foundations and learning algorithms*. The MIT Press, 2017.
- JM Robins, MA Hernán, G Fitzmaurice, M Davidian, G Verbeke, and G Molenberghs. Longitudinal data analysis. *Handbooks of modern statistical methods*, pages 553–599, 2009.
- Gabriele Schweikert, Gunnar Rätsch, Christian Widmer, and Bernhard Schölkopf. An empirical analysis of domain adaptation algorithms for genomic sequence analysis. *Advances in neural information processing systems*, 21, 2008.
- Hidetoshi Shimodaira. Improving predictive inference under covariate shift by weighting the log-likelihood function. *Journal of statistical planning and inference*, 90(2):227–244, 2000.

Samy Suissa. Immortal time bias in pharmacoepidemiology. *American journal of epidemiology*, 167(4): 492–499, 2008.

Katarzyna Tomczak, Patrycja Czerwińska, and Maciej Wiznerowicz. Review the cancer genome atlas (tcga): an immeasurable source of knowledge. *Contemporary Oncology/Współczesna Onkologia*, 2015(1):68–77, 2015.

A Proof of Lemma 2

Convex hulls of finite sets in \mathbb{R}^ℓ are *convex* polytopes, which can be expressed as an intersection of h halfspaces indexed by f with $\{\mathbf{x} : \mathbf{a}^{(f)\top} \mathbf{x} < b^{(f)}\}$ [Grünbaum et al., 1967]. Vectors $\mathbf{a}^{(f)\top}$ can be combined as row-vectors of a matrix, A , so that any convex polytope can be expressed as

$$\{x : A\mathbf{x} < \mathbf{b}\} = \left\{ \mathbf{x} : \begin{pmatrix} (\mathbf{a}^{(1)})^\top \\ \vdots \\ (\mathbf{a}^{(h)})^\top \end{pmatrix} \mathbf{x} < \begin{pmatrix} b^{(1)} \\ \vdots \\ b^{(h)} \end{pmatrix} \right\}. \quad (5)$$

For convenience, the vectors $\mathbf{a}^{(f)}$, $\tilde{\mathbf{a}}^{(f)}$ are assumed to be unit vectors throughout.

The idea behind the proof will be to analyze the movement of the boundaries of the polytope defined by $V = \{\mathbf{v}_1, \dots, \mathbf{v}_m\}$ and corresponding polytope defined by the “perturbed points” $\tilde{V} = \{\tilde{\mathbf{v}}_1, \dots, \tilde{\mathbf{v}}_m\}$. They key is to show that a point that is far enough from the boundary of $\text{Co}(V)$ will also be within $\text{Co}(\tilde{V})$, given by Lemma 4. This required distance from the boundary will be relative to the amount by which the perturbed points have moved. As we bring the perturbation arbitrarily small (i.e. $\varepsilon \rightarrow 0$, all points in the interior of the polytope will be included.

Lemma 4. *Let*

$$\begin{aligned} \text{Co}(V) &= \{\mathbf{x} : A\mathbf{x} < \mathbf{b}\} \\ \text{Co}(\tilde{V}) &= \{\mathbf{x} : \tilde{A}\mathbf{x} < \tilde{\mathbf{b}}\} \end{aligned}$$

as given by Equation 5. If $A\mathbf{x} < \mathbf{b} - \varepsilon \mathbf{1}^\ell$ and $\|\mathbf{v}_i - \tilde{\mathbf{v}}_i\|_2 < \varepsilon \forall i$, then $\tilde{A}\mathbf{x} < \tilde{\mathbf{b}}$.

To prove Lemma 4, we will need to show that the boundaries of the polytopes do not move too much. We will do this using Lemma 5, which bounds how far $\text{Bo}(\text{Co}(V))$ can be from $\text{Bo}(\text{Co}(\tilde{V}))$ along a single “face.”

Definition 7. Choose $f \in [h]$. Define:

$$\begin{aligned} W^{(f)} &= \{\mathbf{w} : (\mathbf{a}^{(f)})^\top \mathbf{w} = b^{(f)}, \mathbf{w} \in V\} \\ \tilde{W}^{(f)} &= \{\tilde{\mathbf{v}}_i : \mathbf{v}_i \in W^{(f)}\} \end{aligned}$$

We restrict the size of $|W^{(f)}| = \ell$, which is the number of points needed to define a halfspace in \mathbb{R}^ℓ . This can be done by allowing for multiple identical \mathbf{a}_f, b_f combinations corresponding to all size ℓ subsets of the v_i along the boundary.

Note that $\text{Co}(W^{(f)})$ describes a “face” of the polytope $\text{Co}(V)$ indexed by f which is perpendicular to $\mathbf{a}^{(f)}$. $\text{Co}(\tilde{W}^{(f)})$ describes the perturbed face.

Lemma 5. *Choose $f, g \in [h]$ arbitrarily and let $W^{(f)} = \{\mathbf{w}_1^{(f)}, \dots, \mathbf{w}_\ell^{(f)}\}$ and $\tilde{W}^{(f)} = \{\tilde{\mathbf{w}}_1^{(f)}, \dots, \tilde{\mathbf{w}}_\ell^{(f)}\}$. For every $\mathbf{m}^{(f)} \in \overline{\text{Co}(W^{(f)})}$, we have $(\tilde{\mathbf{a}}^{(g)})^\top \mathbf{m}^{(f)} < \tilde{b}^{(g)} + \varepsilon$.*

Proof. Because $m \in \overline{\text{Co}(W^{(f)})}$, there is some $\lambda \in \Delta_\ell$ with

$$\mathbf{m}^{(f)} = \sum_{i=1}^{\ell} \lambda_i \mathbf{w}_i^{(f)} \in \overline{\text{Co}(W^{(f)})} \quad (6)$$

Consider also

$$\tilde{\mathbf{m}}^{(f)} = \sum_{i=1}^{\ell} \lambda_i \tilde{\mathbf{w}}_i^{(f)} \in \overline{\text{Co}(\tilde{W}^{(f)})} \quad (7)$$

Note that the norm of the difference between these two vectors is bounded:

$$\begin{aligned} \left\| \mathbf{m}^{(f)} - \tilde{\mathbf{m}}^{(f)} \right\|_2 &= \left\| \sum_{i=1}^{\ell} \lambda_i (\mathbf{w}_i^{(f)} - \tilde{\mathbf{w}}_i^{(f)}) \right\|_2 \\ &\leq \sum_{i=1}^{\ell} \lambda_i \underbrace{\left\| \mathbf{w}_i^{(f)} - \tilde{\mathbf{w}}_i^{(f)} \right\|_2}_{< \varepsilon} < \varepsilon \end{aligned} \quad (8)$$

Also note that because $\tilde{\mathbf{m}}^{(f)} \in \overline{\text{Co}}(\tilde{W}^{(f)}) \subseteq \overline{\text{Co}}(\tilde{V})$, we have that $(\tilde{\mathbf{a}}^{(g)})^\top \tilde{\mathbf{m}}^{(f)} \leq \tilde{b}^{(g)}$. Now, a simple application of Cauchy-Schwartz gives:

$$\begin{aligned} (\tilde{\mathbf{a}}^{(g)})^\top \mathbf{m}^{(f)} &= (\tilde{\mathbf{a}}^{(g)})^\top (\tilde{\mathbf{m}}^{(f)} + (\mathbf{m}^{(f)} - \tilde{\mathbf{m}}^{(f)})) \\ &= \underbrace{(\tilde{\mathbf{a}}^{(g)})^\top \tilde{\mathbf{m}}^{(f)}}_{\leq \tilde{b}^{(g)}} + (\tilde{\mathbf{a}}^{(g)})^\top (\mathbf{m}^{(f)} - \tilde{\mathbf{m}}^{(f)}) \\ &\leq \tilde{b}^{(g)} + \left\| \tilde{\mathbf{a}}^{(g)} \right\|_2 \left\| \mathbf{m}^{(f)} - \tilde{\mathbf{m}}^{(f)} \right\|_2 \\ &< \tilde{b}^{(g)} + \varepsilon \end{aligned} \quad (9)$$

□

With this, we are now ready to prove Lemma 4.

Proof. Choose an arbitrary face $g \in [h]$. Recall we have $\mathbf{x} \in \text{Co}(V)$ with $(\mathbf{a}^{(g)})^\top \mathbf{x} < b - \varepsilon$ and we wish to show $(\tilde{\mathbf{a}}^{(g)})^\top \mathbf{x} < \tilde{b}^{(g)}$.

Let $\mathbf{m}_x^{(f)}$ be the result of extending $\tilde{\mathbf{a}}^{(g)}$ from \mathbf{x} to $\text{Bo}(V)$. This must hit some face with $(\mathbf{a}^{(f)})^\top \mathbf{m}_x^{(f)} = b^{(f)}$, so $\mathbf{m}_x^{(f)} \in \text{Co}(W^{(f)})$. That is, find β such that

$$\mathbf{m}_x^{(f)} = \beta \tilde{\mathbf{a}}^{(g)} + \mathbf{x} \in \text{Co}(W^{(f)}) \quad (10)$$

First, lets bound β . Notice that because $\mathbf{m}_x^{(f)} \in \text{Co}(W^{(f)})$, we have

$$\begin{aligned} (\mathbf{a}^{(f)})^\top \mathbf{m}_x^{(f)} &= (\mathbf{a}^{(f)})^\top \left(\sum_{i=1}^{\ell} \lambda_i \mathbf{w}_i^{(f)} \right) \\ &= \sum_{i=1}^{\ell} \lambda_i (\mathbf{a}^{(f)})^\top \mathbf{w}_i^{(f)} = b^{(f)} \end{aligned} \quad (11)$$

So, we have

$$b^{(f)} = (\mathbf{a}^{(f)})^\top \mathbf{m}_x^{(f)} = \beta \underbrace{(\mathbf{a}^{(f)})^\top \tilde{\mathbf{a}}^{(g)}}_{\leq 1} + \underbrace{(\mathbf{a}^{(f)})^\top \mathbf{x}}_{< b^{(f)} - \varepsilon} \Rightarrow \varepsilon < \beta \quad (12)$$

Now, apply Lemma 5

$$\begin{aligned} (\tilde{\mathbf{a}}^{(g)})^\top \mathbf{m}_x^{(f)} &< \tilde{b}^{(g)} + \varepsilon \\ (\tilde{\mathbf{a}}^{(g)})^\top \mathbf{x} + (\tilde{\mathbf{a}}^{(g)})^\top \tilde{\mathbf{a}}^{(g)} \beta &< \tilde{b}^{(g)} + \varepsilon \\ (\tilde{\mathbf{a}}^{(g)})^\top \mathbf{x} &< \tilde{b}^{(g)}. \end{aligned} \quad (13)$$

Face $g \in [h]$ was chosen arbitrarily, so this holds for all halfspaces in the convex polytope. Hence, we have $A\mathbf{x} < \mathbf{b}$. □

B Counts that Follow the Correct DAG

The paradox presented in Table 1 (c) used counts yielding a distribution that does not precisely follow the given DAG. We will now show how to construct a similar set of counts with the statistics needed to imply the causal structure.

T	X	$y^{(0)}$	$y^{(1)}$	$y^{(2)}$
$t^{(1)}$	$x^{(1)}$	$2\alpha_1$	α_1	0
$t^{(1)}$	$x^{(2)}$	0	$2\beta_1$	β_1
$t^{(1)}$	$x^{(3)}$	γ_1	0	$2\gamma_1$
$t^{(0)}$	$x^{(1)}$	0	α_2	$2\alpha_2$
$t^{(0)}$	$x^{(2)}$	$2\beta_2$	0	β_2
$t^{(0)}$	$x^{(3)}$	γ_2	$2\gamma_2$	0

Table 2: A more general specification of counts for our paradox.

Consider Table 2. The structure is copied from Table 1 (c). If $\alpha_1 = \alpha_2$, $\beta_1 = \beta_2$, and $\gamma_1 = \gamma_2$, then we notice that the relative probabilities of $\Pr(x)$ are given by the α s, β s, and γ s. If these coefficients are all equal, then we have every row considered with equal weight, as in the main paper.

While setting all of the Greek coefficients to 1 provides a nice intuition for how the paradox emerges, it unfortunately does not give a distribution that obeys the requirements of the given DAG. In order for our distribution to (1) factorize according to the DAG and (2) be faithful to the DAG, we must have the following properties:

1. $T \not\perp\!\!\!\perp Y$
2. $X \not\perp\!\!\!\perp Y$
3. $T \not\perp\!\!\!\perp X$
4. $T \not\perp\!\!\!\perp Y \mid X$
5. $X \not\perp\!\!\!\perp Y \mid T$
6. $T \not\perp\!\!\!\perp X \mid Y$

With all of the Greek coefficients set to 1, we notice that conditions 5,6 are met. The domain expertise setting effectively conditions on Y by restricting it's values. When restricted to two columns, we also meet condition 4.

The remaining conditions (as well as condition 4 in the broader case) can be met by varying the Greek coefficients. Attached code allows one to explore different settings to the Greek coefficients to achieve this paradox. One example is $\alpha_1 = \beta_1 = \gamma_1 = 1$ and $\alpha_2 = 1.1$, $\beta_2 = 1.2$, $\gamma_2 = 1.3$. The code is a Jupyter python notebook that allows one to define a probability table using the given Greek coefficients and check whether the 6 independence conditions hold. The three ATEs for each omitted label context are then printed. All code was run on Macbook air with an M1 processor.